

---

# NFISIS: NEW PERSPECTIVES ON FUZZY INFERENCE SYSTEMS FOR RENEWABLE ENERGY FORECASTING

---

A PREPRINT

✉ **Kaike Sa Teles Rocha Alves**  
Computational Modeling  
Federal University of Juiz de Fora  
Juiz de Fora, MG  
kaike.alves@outlook.com

✉ **Eduardo Pestana de Aguiar**  
Department of Industrial and Mechanical Engineering  
Federal University of Juiz de Fora  
Juiz de Fora, MG  
eduardo.aguiar@ufjf.br

June 27, 2025

## ABSTRACT

Deep learning models, despite their popularity, face challenges such as long training times and a lack of interpretability. In contrast, fuzzy inference systems offer a balance of accuracy and transparency. This paper addresses the limitations of traditional Takagi-Sugeno-Kang fuzzy models by extending the recently proposed New Takagi-Sugeno-Kang model to a new Mamdani-based regressor. These models are data-driven, allowing users to define the number of rules to balance accuracy and interpretability. To handle the complexity of large datasets, this research integrates wrapper and ensemble techniques. A Genetic Algorithm is used as a wrapper for feature selection, creating genetic versions of the models. Furthermore, ensemble models, including the Random New Mamdani Regressor, Random New Takagi-Sugeno-Kang, and Random Forest New Takagi-Sugeno-Kang, are introduced to improve robustness. The proposed models are validated on photovoltaic energy forecasting datasets, a critical application due to the intermittent nature of solar power. Results demonstrate that the genetic and ensemble fuzzy models, particularly the Genetic New Takagi-Sugeno-Kang and Random Forest New Takagi-Sugeno-Kang, achieve superior performance. They often outperform both traditional machine learning and deep learning models while providing a simpler and more interpretable rule-based structure. The models are available online in a library called nfisis (<https://pypi.org/project/nfisis/>).

**Keywords** Fuzzy inference systems · Time series forecasting · Feature selection · Genetic algorithm · Ensemble

## 1 Introduction

Deep learning (DL) techniques have become increasingly popular due to technological advances and the growing complexity of databases. However, DL models are more intricate and susceptible to several issues, such as vanishing gradients, overfitting, long training times Shrestha and Mahmood [2019], and the inability to provide interpretable results due to their black-box nature Wang et al. [2020], Rai [2020]. In contrast, fuzzy inference systems (FIS), represent a class of machine learning models that combine accuracy with interpretability. These systems are primarily divided into two categories: Mamdani Mamdani [1974] and Takagi-Sugeno-Kang (TSK) Takagi and Sugeno [1985], Sugeno and Kang [1988]. These systems have been successfully applied in various fields, including finance, business, and management Bojadziev and Bojadziev [2007], medicine Szczepaniak and Lisboa [2012], engineering Precup and Hellendoorn [2011], chemistry Komiyama et al. [2017], pattern recognition Melin et al. [2011], and fault detection Lemos et al. [2013]. However, Alves et al. Alves et al. [2024], Sa Teles Rocha Alves et al. [2024] identified several limitations in TSK models, including: i) a lack of a unique approach for defining TSK rules; ii) data-driven TSK models are usually more complex, have many hyper-parameters, and involve hybridizations; iii) there is no direct control over the number of rules in data-driven approaches; and iv) the consequent part of TSK models lacks explainability, as it consists of polynomial functions. To address these limitations, the authors proposed the New Takagi-Sugeno-Kang (NTSK) model.

NTSK is a data-driven fuzzy model with reduced complexity and increased interpretability. Alves et al. also highlight the following: first, the number of rules is a hyper-parameter, allowing the user to set the exact number of rules that balance the trade-off between accuracy and interpretability. Second, the model defines the rules based on the tangent of the target value. This additional information enhances the interpretability of the consequent part. Finally, the approach has a reduced number of hyper-parameters and lower complexity, making it suitable for use in various real-world applications. The simulations demonstrated the superior performance of the proposed model, surpassing the performance of more complex models, such as DL.

In this paper, the concepts of NTSK will be extended to a new Mamdani fuzzy inference system (NMFIS) called the new Mamdani regressor (NMR). NMR is an autonomous model that defines the rule-based structure from data using a data-driven approach. The only requirement is to specify the desired number of rules. Like NTSK, NMR automatically defines the fuzzy sets and rules, offering a simple structure and accurate results, making it suitable for implementation in real-world applications. Nevertheless, with the growing complexity of databases, one challenge remains: which attributes should be selected to optimize the model's performance while considering the trade-off between accuracy and interpretability? The answer to this question depends on feature selection techniques, which can be divided into five main types: filter, wrapper, embedded, hybrid, and ensemble Zebari et al. [2020].

Filter methods are a statistic-based approach, but they neglect the integration between the selected subset and the performance of the learning algorithm Eesa et al. [2015]. In contrast, wrapper methods use a metric that measures the learning algorithm's performance to identify the feature set that leads to the best results. However, since it is infeasible to test all possible combinations of features, heuristic and metaheuristic approaches are employed, such as randomized search Mao and Yang [2019], genetic algorithm (GA) Sohail [2023], and the ant colony optimization Forsati et al. [2014]. In embedded methods, the feature selection technique is integrated into the learning algorithm by adjusting the model's internal parameters. Decision trees, random forests, and gradient boosting are examples of embedded feature selection techniques Guyon and Elisseeff [2003]. Hybrid methods combine multiple feature selection approaches in a multi-step process Hsu et al. [2011]. Finally, an ensemble learner implements multiple weak learning algorithms and combines their results to achieve better performance than any individual model Bolón-Canedo and Alonso-Betanzos [2019], Dong et al. [2020].

Considering this, this paper combines a wrapper and an ensemble technique with the proposed NFISiS to enhance the models' ability to handle large datasets, optimize their performance, and increase interpretability, as only the most important features will be selected. The wrapper technique uses a GA to search for the combination of attributes that minimizes errors. These models are referred to as genetic NMR (GEN-NMR), genetic NTSK-RLS (GEN-NTSK-RLS), and genetic NTSK-wRLS (GEN-NTSK-wRLS). In addition, the Random NMR (R-NMR), Random NTSK (R-NTSK), and Random Forest NTSK (RF-NTSK) are introduced, all of which are ensemble models. The R-NMR and R-NTSK are ensemble versions of the NMR and NTSK models, respectively. On the other hand, RF-NTSK combines the outputs of R-NTSK and RF to compute the final result. The models are applied to renewable energy datasets. Such a series was chosen because of their complexity and relevance in many real-world applications. The models are applied to renewable energy datasets. These datasets were chosen due to their complexity and relevance in various real-world applications.

Photovoltaic (PV) energy is expected to become one of the primary sources of energy worldwide in the future, as it is abundant, affordable, and easily scalable Alcañiz et al. [2023]. However, the energy supplied by PV modules can be intermittent due to the varying nature of weather conditions Notton et al. [2018]. Forecasting the power generated in a PV plant is crucial, as it helps grid operators, plant managers, and energy markets anticipate and manage the variability inherent in PV energy generation. Accurate forecasts optimize energy production, ensure a stable and reliable power supply, and contribute to cost reduction, efficient resource planning, and the overall sustainability of the energy landscape. Furthermore, the chaotic nature and uncertainties associated with PV energy make it difficult to obtain accurate results using physical equations, which has led to the increased use of machine learning models for predicting PV energy generation Mayer and Gróf [2021].

Given the critical importance of PV energy control, numerous researchers have addressed this topic extensively. Wan et al. [2015], Barbieri et al. [2017], Das et al. [2018], Alcañiz et al. [2023] presented an extensive literature review on this topic. Munsif et al. [2023] proposed the convolutional-transformer-based network (CT-NET) for power forecasting. Jailani et al. [2023] implement LSTM for solar energy. Artificial neural networks (ANN) Khandakar et al. [2019], ANN with feature selection O'Leary et al. [2017] was also discussed. Sharma et al. [2023] utilized a Levenberg Marquardt artificial neural network (LM-ANN) that uses the gradient descent (GD) optimization technique for solar energy forecasting. Among the advantages of using ANNs, the following can be highlighted: (i) self-adaptive ability; (ii) fault-tolerance; (iii) robustness; and (iv) strong inference capabilities Yang et al. [2014]. However, due to the architecture of ANNs, they can present increased complexity. Support Vector Machines (SVM) have also been explored for PV energy forecasting Preda et al. [2018], praised for their non-linear modeling capacity and independence from prior knowledge Li et al.

[2016]. Numerous hybrid approaches using SVM have emerged, such as PSO-SVM Eseye et al. [2018], GASVM VanDeventer et al. [2019], SVM with an improved ant colony optimization (ACO-SVM). TSK-based models have some applications to the power predictions of PV systems Liu et al. [2017, 2021]. A remarkable advantage of fuzzy models is their ability to handle uncertainties in real-world data Ghofrani et al. [2016]. Still discussing fuzzy models, ANFIS usually presents errors substantially lower than those of fuzzy models. However, the computational complexity also increases, especially compared to SVM Das et al. [2018], Law et al. [2014].

The remainder of this paper is organized as follows: Section 2 presents in detail the background knowledge on NTSK. Section 3 introduces and discusses the proposed models, presenting the mathematical formalism. Section 4 shows the simulations and discusses the results. Finally, Section 5 concludes the paper and proposes future works.

## 2 Background Knowledge on NTSK

The steps to define the NTSK rules are as follows:

- **Step 1 - Define the Number of Rules:** Specify the maximum number of rules ( $R_{\max}$ ) as a hyper-parameter.
- **Step 2 - Compute Target Value Variations:** Calculate the variation in the target values for all samples.
- **Step 3 - Define Intervals for Variations:** Create equally spaced intervals based on the range of target value variations and  $R_{\max}$ .
- **Step 4 - Assign Samples to Rules:** Assign samples to the corresponding rule based on their variation intervals.
- **Step 5 - Compute Fuzzy Sets:** Determine the parameters of the fuzzy sets (e.g., the mean and standard deviation for Gaussian membership functions).
- **Step 6 - Compute Consequent Parameters:** Estimate the consequent parameters using an adaptive filtering approach.

The flowchart for the NTSK training phase is presented in Figure 1.

## 3 The Proposed Models

This section introduces the proposed models. Initially, the NMR is described and analyzed. Subsequently, the integration of GA and ensemble methods with NMR is presented and discussed.

### 3.1 The New Mamdani Regressor (NMR)

NMR is a data-driven fuzzy logic approach that constructs rules by defining intervals based on the target values. During the training phase, the model creates equally spaced intervals for the target variable to define the rules, subsequently determining the fuzzy sets for the antecedent part. The process is summarized as follows:

**Step 1 - Define the Number of Rules:** The user specifies the desired number of rules.

**Step 2 - Define Intervals for Target Values:** The model computes the amplitude of the target values and divides the result by the number of rules to create equally spaced intervals.

**Step 3 - Define the Rules:** Each interval corresponds to one rule.

**Step 4 - Assign Samples to Rules:** Samples are assigned to the rule where the target value falls within the interval.

**Step 5 - Compute the Fuzzy Sets:** Fuzzy sets are generated for the antecedent and consequent parts.

Figure 2 illustrates the steps in the training phase of NMR. Once trained, the model is ready for inference.

#### 3.1.1 Defining NMR Rules - Training Phase

This part presents the mathematics and formalities of defining the rules. First, the user informs the desired number of rules, referred to as  $R_{\max}$ . After that, the algorithm computes the interval size (IS) as a function of the target values' amplitude and  $R_{\max}$ , as presented below:

$$IS = \frac{\bar{y} - y}{R_{\max}} \quad (1)$$

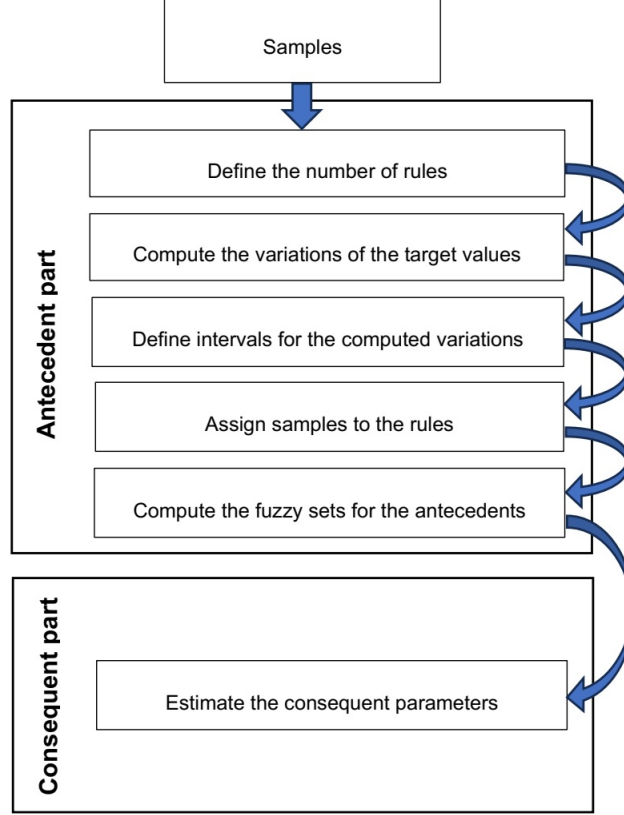


Figure 1: Flowchart presenting the learning phase for NTSK

where  $IS$  means the range interval for the target value,  $\bar{y}$  is the target's maximum value,  $\underline{y}$  is the target's minimum value, and  $R_{max}$  is a hyper-parameter that defines the model's number of rules.

The  $IS$  is used to compute each interval for the consequent part of all rules, as shown in Equation (2). The model assigns the samples to the rules based on the target value. So, for example, if the interval of the consequent part for the first rule is  $[1, 3]$ , it means that the first rule comprises samples with a target value between one and three.

$$Range_i = [\underline{y} + (i - 1)IS, \underline{y} + (i)IS] \quad (2)$$

where  $Range_i$  represents the interval of the consequent part of the  $i$ th rule and  $i = 1, 2, \dots, R_{max}$  is the rule number.

Defined the intervals of the consequent part of each rule, the next step consists of assigning the samples to their respective rule by comparing the target value with the intervals. Equation (3) presents a formula to identify which rule the  $k$ th sample will be assigned.

$$i_{S^k} = \begin{cases} \lfloor \frac{y^k - \underline{y}}{IS} \rfloor, & \text{if } y^k < \bar{y} \\ R_{max}, & \text{otherwise} \end{cases} \quad (3)$$

where  $i_{S^k}$  is the rule in which the  $k$ th sample will be included and  $\lfloor \cdot \rfloor$  represents the floor function.

Finally, the last step of defining the rules is to compute the fuzzy sets for the antecedent and consequent parts. Gaussian fuzzy sets are implemented in this paper (see Equation (4)). Only two parameters are required for Gaussian fuzzy sets: the mean and the standard deviation.

$$\mu_A(x) = \exp \left[ -\frac{1}{2} \left( \frac{x - v}{\sigma} \right)^2 \right] \quad (4)$$

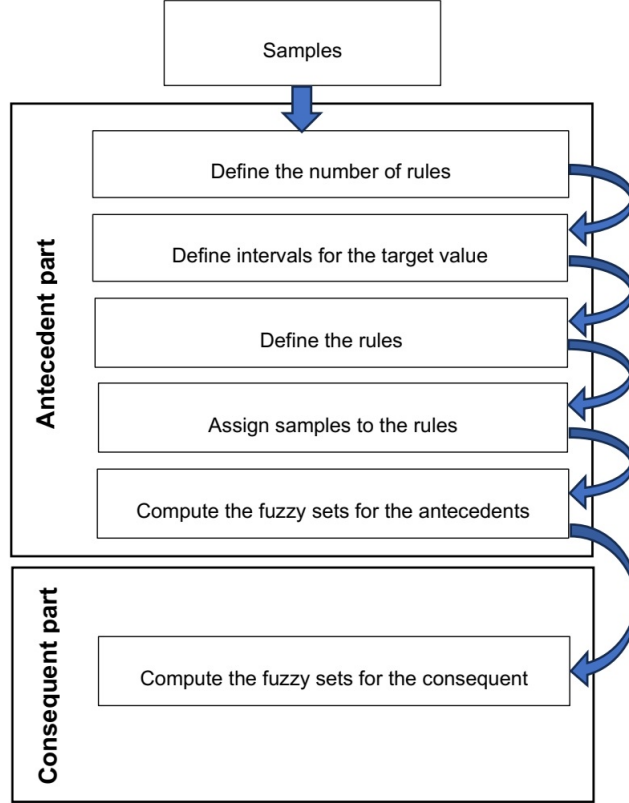


Figure 2: Flowchart of the learning phase for NMR

where  $v$  represents the mean of the fuzzy set and  $\sigma$  is the standard deviation. Gaussian membership functions are advantageous because they are smooth, non-zero over all points, and effectively represent linguistic variables with precision and clarity Azimi and Miar-Naimi [2020].

### 3.1.2 The Inference Process for NMR - Test Phase

First, the input data is fuzzified using the respective membership functions. Then, each fuzzified input must be combined using a fuzzy operator to compute the normalized firing degree for each rule (Equation (5)). The rule with a higher degree of activation informs a higher degree of pertinence with the respective input.

$$w_i = \frac{\prod_{j=1}^p \exp \left[ -\frac{1}{2} \frac{(x_j^k - v_{i,j})^2}{\sigma_{i,j}^2} \right]}{\sum_{i=1}^R \left( \prod_{j=1}^p \exp \left[ -\frac{1}{2} \frac{(x_j^k - v_{i,j})^2}{\sigma_{i,j}^2} \right] \right)} \quad (5)$$

where  $v_{i,j}$  is mean of the  $j$ th attribute for the  $i$ th rule,  $v_i = [v_{i,1}, \dots, v_{i,p}]^T$ ,  $p$  is the dimension of the inputs (number of attributes for each sample),  $x_j^k$  is the  $k$ th input vector for the  $j$ th attribute, and  $\sigma_{i,j}$  is the standard deviation of the  $j$ th attribute for the  $i$ th rule, for  $\sigma_i = [\sigma_{i,1}, \dots, \sigma_{i,p}]^T$ .

Finally, defuzzification can occur, which consists of computing the model's output according to Equation (6).

$$\hat{y}^k = \frac{\sum_{i=1}^{R_{max}} v_{i,output} \times w_i}{\sum_{i=1}^{R_{max}} w_i} \quad (6)$$

where  $v_{i,output}$  is mean of the consequent fuzzy set for the  $i$ th rule.

The concepts of NMR can easily be expanded to the new Mamdani classifier (NMC), but instead of having the number of rules defined by the user, it will be related to the number of classes the data have. Each class will constitute a rule. However, it will not be discussed here.

### 3.1.3 Genetic Algorithm Implementation

This section presents the implementation of the Genetic Algorithm (GA) for feature selection. Initially, the dataset is divided into training and testing subsets. A binary vector, whose length corresponds to the number of attributes, is then created to represent feature selection. Each position in the vector indicates whether the corresponding attribute is included (1) or excluded (0) in the feature subset. To ensure at least one attribute is always selected, the vector must contain at least one nonzero element; otherwise, no attributes would be chosen.

Once the initial population of vectors is generated, the algorithm evaluates their fitness by invoking the fuzzy model. The fitness assessment is based on the model's performance using the selected features. The GA iteratively evolves the population until the termination criteria are met. At the end of the process, the vector yielding the lowest error is saved as the optimal feature subset.

## 3.2 Ensemble Fuzzy

This section introduces three ensemble fuzzy models: R-NMR, R-NTSK, and RF-NTSK. The R-NMR and R-NTSK models operate similarly, employing a randomized approach to attribute selection. In both models, a subset of attributes is randomly selected from the original dataset, and  $z$  models are trained. The best-performing model from this subset is added to the ensemble, after which the process is repeated to identify additional models until the desired number of inducers is obtained.

Finally, RF-NTSK acts as an ensemble of ensembles, combining the outputs of RF and NTSK. The final prediction is calculated using Equation (7), which assigns weights to each output based on their respective errors.

$$\hat{y}^k = \hat{y}_{RF}^k \frac{\epsilon_{R-NTSK}}{\epsilon_{RF} + \epsilon_{R-NTSK}} + \hat{y}_{R-NTSK}^k \frac{\epsilon_{RF}}{\epsilon_{RF} + \epsilon_{R-NTSK}} \quad (7)$$

where  $\epsilon_{RF}$  and  $\epsilon_{R-NTSK}$  are the estimated error of RF and R-NTSK during the training phase, respectively, and  $\hat{y}_{RF}^k$  and  $\hat{y}_{R-NTSK}^k$  the output of RF and R-NTSK, respectively. It can be seen that the output is a weighted average of the output of RF and R-NTSK where the weights are inversely proportional to the errors.

## 4 Experimental Results and Discussion

This section presents the metrics employed to evaluate the simulations and shows and discusses the results.

### 4.1 Evaluation Indicators

The model's performance is assessed using the normalized root-mean-square error (NRMSE), the non-dimensional index error (NDEI), and the mean absolute percentage error (MAPE), defined by Equations (8), (9), and (10), respectively.

$$NRMSE = \frac{RMSE}{\bar{y} - \underline{y}} \quad (8)$$

$$NDEI = \frac{RMSE}{std([y^1, \dots, y^T])} \quad (9)$$

$$MAPE = \frac{1}{T} \sum_{k=1}^T \frac{\|y^k - \hat{y}^k\|}{y^k} \quad (10)$$

where  $y^k$  is the  $k$ th actual value,  $\hat{y}^k$  is the  $k$ th predicted value,  $\bar{y}$  is the maximum value for  $y$ ,  $\underline{y}$  is the minimum value for  $y$ ,  $T$  is the sample size, and  $std()$  is the standard deviation function, and RMSE is the root-mean-square error given in Equation (11).

$$RMSE = \sqrt{\frac{1}{T} \sum_{k=1}^T (y^k - \hat{y}^k)^2} \quad (11)$$

RMSE is largely used in the literature due to its advantages, such as being sensitive to outliers, suitable for optimizations, and allowing comparison between different models. To improve the visualization, the paper reports the normalized NRMSE, which normalizes the RMSE by the amplitude. Furthermore, the NDEI is commonly used in the literature to evaluate eFS models. This metric informs how many times the RMSE is concerning the standard deviation of the data. On the other hand, the MAPE is less sensitive to outliers, but it is suitable in cases where the percentage error is more relevant than absolute errors.

For rule-based models, the total number of final rules is also reported. The hyper-parameters of the models are optimized through a grid search to achieve the lowest possible error.

Additionally, two statistical tests are employed to analyze the linearity and stationarity of real-world time series: the Shapiro-Wilk test Shapiro and Wilk [1965] and the augmented Dickey-Fuller (ADF) test Dickey and Fuller [1981]. While the derivations of these tests are beyond the scope of this work, detailed explanations can be found in the literature.

For the Shapiro-Wilk test, a  $p$ -value less than 0.05 rejects the null hypothesis, indicating that the series does not originate from a normal distribution. Conversely, a  $p$ -value greater than 0.05 suggests that the series follows a normal distribution. Similarly, the ADF test interprets a  $p$ -value below 0.05 as evidence supporting stationarity, while a  $p$ -value exceeding 0.05 implies non-stationarity.

## 4.2 Datasets

Finally, PV energy datasets from two power plants, Alice Springs and Yulara Solar System, are implemented. Desert Knowledge Australia Solar Centre (DKASC) Alice Springs is a giant solar energy power station located in the Alice Springs desert that contains PV technologies of different types, ages, makes, models, and configurations. Operating since 2008, Alice offers a vast database for researchers. This work aims to predict the daily power one step ahead using as predictors the following attributes: humidity, diffuse radiation, radiation, diffuse tilted, accumulated energy, rainfall, wind direction, temperature, radiation global, tilted, energy, global radiation, power, and the current.

On the other hand, the Yulara Solar System, installed in 2014, is located near Yulara and operates a 1.8 MW solar photovoltaic plant. Two datasets from Yulara are implemented to predict the daily power one step ahead using as predictors air pressure, wind direction, rainfall, hail, wind speed, accumulated energy, max wind speed, pyranometer, global radiation, temperature, temperature probe 1, temperature probe 2, energy, power, and the current. More information about these attributes can be found on the website. The PV panels Yulara 1 and 5 were chosen to perform the simulations. The initial dataset contained information in the 5-minute interval. Pre-processing was implemented to remove null values and convert the information to daily values. The datasets' period includes data from January 2021 to December 2022.

More information about the datasets can be found on the official website: <https://dkasolarcentre.com.au/>. As the plant uses solar panels with different characteristics, the panels are identified by numbers. Table 1 presents the characteristics of PV panels, and Table 2 shows the statistical results for the datasets. The results suggest that only Yulara 5 comes from a normal distribution and that all datasets are stationary.

Table 1: Characteristics of the PV panels implemented in the simulations

Characteristics	Alice 1A	Alice 38	Yulara 1	Yulara 5
Manufacturer	Trina	Q CELLS	-	-
Array Rating	10.5kW	5.9kW	1058.4kW	105.9kW
PV Technology	mono-Si	mono-Si	poly-Si	mono-Si
Array Structure Tracker	Dual Axis	Ground Mount	Ground Mount	Roof Mount
Installed	2009	2017	2016	2016

## 4.3 Results

Table 3 presents the simulations' results for the Alice 1A time series. SVM and LS-SVM obtained the lowest errors among the classical models, LSTM the lowest among DL models, eTS and ePL+ the lowest for the eFSs, and GEN-

Table 2: Statistical tests of the PV energy datasets

Test	Alice 1A	Alice 38	Yulara 1	Yulara 5
Shapiro-Wilk	$5.0 \times 10^{-17}$	$1.4 \times 10^{-27}$	$5.4 \times 10^{-11}$	0.37
ADF	$8.5 \times 10^{-8}$	$1.0 \times 10^{-20}$	$3.7 \times 10^{-20}$	$8.3 \times 10^{-4}$

NTSK (wRLS) and R-NTSK for the proposed fuzzy models. Furthermore, eTS obtained the lowest NRMSE and NDEI among all simulations and ePL+ the lowest MAPE, supporting the good performance of the eFSs in real datasets. The ePL, NTSK (RLS), and GEN-NTSK (RLS) achieved the fewest rules and eMG the highest ones. Figure 3 presents the predictions of the lowest NRMSE for each model class for the Alice 1A time series. The models failed to predict some extreme points, which may indicate that the presence of outliers disturbs the predictions.

Table 3: Simulations' results for the Alice 1A PV panel

Model	NRMSE	NDEI	MAPE	Rules
KNN Fix and Hodges [1951]	0.22656	1.00709	0.40166	-
Regression Tree Breiman et al.	0.21325	0.94790	0.37171	-
Random Forest Ho [1995]	0.21480	0.95481	0.36574	-
SVM Cortes and Vapnik [1995]	0.20714	0.92075	<b>0.35383</b>	-
LS-SVM Suykens and Vandewalle [1999]	<b>0.20669</b>	<b>0.91876</b>	0.35509	-
GBM Friedman [2001]	0.21849	0.97119	0.36887	-
XGBoost Chen and Guestrin [2016]	0.21538	0.95736	0.37573	-
LGBM Ke et al. [2017]	0.21320	0.94771	0.37708	-
MLP Rosenblatt [1958]	0.26037	1.15734	0.46606	-
CNN Fukushima [1980]	0.22639	1.00634	0.40184	-
RNN Hopfield [1982]	0.20881	0.92818	0.36124	-
LSTM Hochreiter and Schmidhuber [1997]	<b>0.20776</b>	<b>0.92350</b>	<b>0.35657</b>	-
GRU Chung et al. [2014]	0.26014	1.15636	0.39765	-
WaveNet Oord et al. [2016]	0.25401	1.12910	0.45572	-
eTS Angelov and Filev [2004]	<b>0.20639</b>	<b>0.91742</b>	0.35508	4
Simpl_eTS Angelov and Filev [2005]	0.33692	1.49764	0.43992	56
exTS Angelov and Zhou [2006]	0.20861	0.92729	0.36044	3
ePL Lima et al. [2010]	0.20953	0.93136	0.35760	1
eMG Lemos et al. [2010]	0.40435	1.79734	0.56272	140
ePL+ Maciel et al. [2012]	0.20757	0.92266	<b>0.34947</b>	3
ePL-KRLS-DISCO Alves and de Aguiar [2021]	0.29263	1.30077	0.46094	33
NMR	0.24337	1.08178	0.38902	16
NTSK (RLS)	0.24953	1.10918	0.43855	1
NTSK (wRLS)	0.20957	0.93154	0.35129	4
GEN-NMR	0.23421	1.04108	0.38867	17
GEN-NTSK (RLS)	0.22072	0.98112	0.36194	1
GEN-NTSK (wRLS)	<b>0.20711</b>	<b>0.92061</b>	0.36308	19
R-NMR	0.23220	1.03216	0.36129	-
R-NTSK	0.21431	0.95261	<b>0.35784</b>	-
RF-NTSK	0.21177	0.94132	0.35908	-

Table 4 presents the simulations' results for the Alice 38 time series. LS-SVM obtained the lowest errors among the classical models, CNN and GRU the lowest among DL models, eTS and exTS the lowest for the eFSs, and R-NTSK and RF-NTSK for the proposed fuzzy models. The ePL, NTSK (RLS), and GEN-NTSK (RLS) achieved the fewest final rules, and eMG the highest ones. Figure 4 presents the best predictions of each class for the Alice 38 time series.

Table 5 presents the simulations' results for the Yulara 1 time series. RF obtained the lowest errors among the classical models, CNN among the DL models, eTS and exTS the lowest for the eFSs, and GEN-NMR and RF-NTSK for the proposed fuzzy models. CNN obtained the lowest among all models. The eMG model achieved 189 final rules, the highest among all models. The ePL, ePL+, NTSK (RLS), and GEN-NTSK (RLS) obtained just one final rule. Figure 5 presents the best predictions of each class for the Yulara 1 time series.

Table 6 presents the simulations' results for the Yulara 5 time series. LS-SVM obtained the lowest errors among the classical models, CNN and GRU the lowest among the DL, ePL-KRLS-DISCO the lowest for the eFSs, and GEN-NTSK (wRLS) and R-NTSK the lowest errors for the proposed models. Among all models, ePL-KRLS-DISCO achieved the lowest NRMSE and NDEI, and R-NTSK the lowest MAPE. Simpl\_eTS performed 431 final rules, the highest among



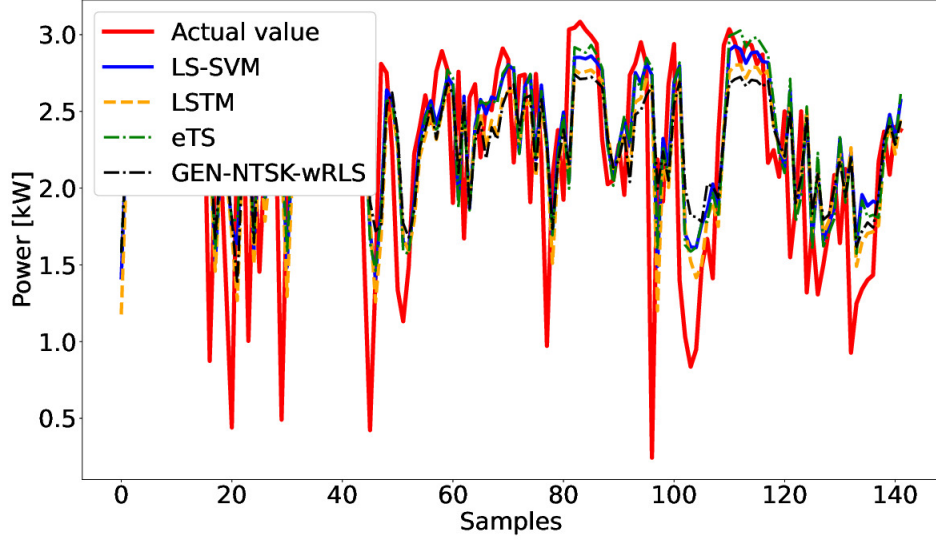


Figure 3: Graphic of predictions for Alice 1A

Table 4: Simulations' results for the Alice 38 PV panel

Model	NRMSE	NDEI	MAPE	Rules
KNN Fix and Hodges [1951]	0.23499	1.04722	0.37156	-
Regression Tree Breiman et al.	0.21404	0.95385	0.34513	-
Random Forest Ho [1995]	0.21363	0.95204	0.34780	-
SVM Cortes and Vapnik [1995]	0.21480	0.95723	0.34494	-
LS-SVM Suykens and Vandewalle [1999]	<b>0.20813</b>	<b>0.92755</b>	<b>0.33040</b>	-
GBM Friedman [2001]	0.25371	1.13065	0.37142	-
XGBoost Chen and Guestrin [2016]	0.22014	0.98103	0.34765	-
LGBM Ke et al. [2017]	0.21548	0.96026	0.34166	-
MLP Rosenblatt [1958]	0.21231	0.94616	0.34199	-
CNN Fukushima [1980]	<b>0.20700</b>	<b>0.92250</b>	0.32452	-
RNN Hopfield [1982]	0.21020	0.93677	0.33125	-
LSTM Hochreiter and Schmidhuber [1997]	0.20858	0.92953	0.33252	-
GRU Chung et al. [2014]	0.21089	0.93981	<b>0.32443</b>	-
WaveNet Oord et al. [2016]	0.25446	1.13400	0.42215	-
eTS Angelov and Filev [2004]	0.21114	0.94093	<b>0.32321</b>	3
Simpl_eTS Angelov and Filev [2005]	0.22844	1.01805	0.34967	36
exTS Angelov and Zhou [2006]	<b>0.20443</b>	<b>0.91105</b>	0.33023	3
ePL Lima et al. [2010]	0.58321	2.59907	0.68757	1
eMG Lemos et al. [2010]	0.28917	1.28866	0.42192	138
ePL+ Maciel et al. [2012]	0.25132	1.11999	0.35191	11
ePL-KRLS-DISCO Alves and de Aguiar [2021]	0.26151	1.16542	0.36657	33
NMR	0.24519	1.09269	0.39498	9
NTSK (RLS)	0.25395	1.13171	0.41610	1
NTSK (wRLS)	0.23656	1.05424	0.35931	11
GEN-NMR	0.26173	1.16638	0.35348	13
GEN-NTSK (RLS)	0.21581	0.96176	0.34244	1
GEN-NTSK (wRLS)	0.25224	1.12411	0.36122	13
R-NMR	0.21897	0.97582	0.33655	-
R-NTSK	0.21150	0.94252	<b>0.33032</b>	-
RF-NTSK	<b>0.21087</b>	<b>0.93974</b>	0.33716	-

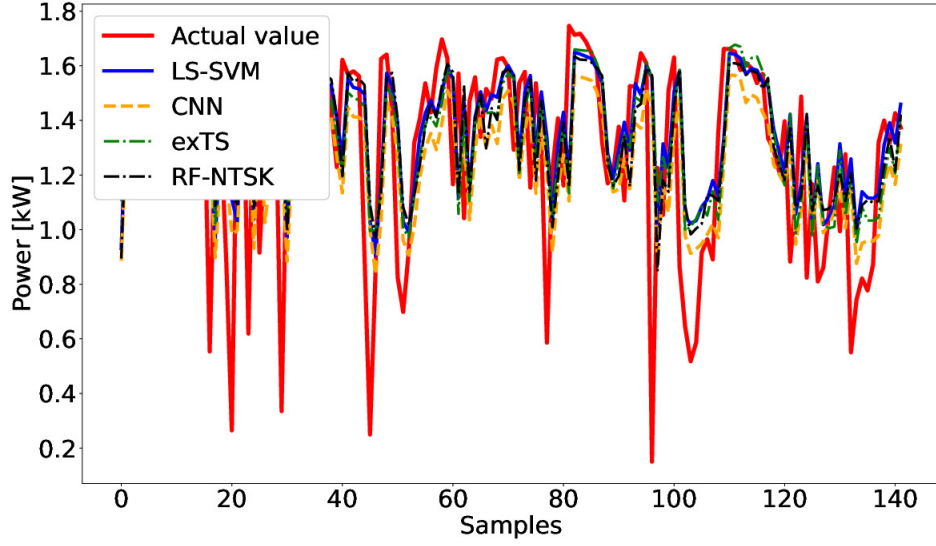


Figure 4: Graphic of predictions for Alice 38

Table 5: Simulations' results for the Yulara 1 PV panel

Model	NRMSE	NDEI	MAPE	Rules
KNN Fix and Hodges [1951]	0.21399	1.02255	0.39364	-
Regression Tree Breiman et al.	0.21037	1.00523	0.28632	-
Random Forest Ho [1995]	<b>0.17592</b>	<b>0.84064</b>	<b>0.27256</b>	-
SVM Cortes and Vapnik [1995]	0.21055	1.00610	0.34657	-
LS-SVM Suykens and Vandewalle [1999]	0.21319	1.01869	0.36743	-
GBM Friedman [2001]	0.18105	0.86514	0.29454	-
XGBoost Chen and Guestrin [2016]	0.20440	0.97670	0.30765	-
LGBM Ke et al. [2017]	0.17896	0.85515	0.28816	-
MLP Rosenblatt [1958]	0.17511	0.83676	0.26667	-
CNN Fukushima [1980]	<b>0.16568</b>	<b>0.79168</b>	<b>0.25176</b>	-
RNN Hopfield [1982]	0.22641	1.08191	0.29806	-
LSTM Hochreiter and Schmidhuber [1997]	0.24267	1.15959	0.29554	-
GRU Chung et al. [2014]	0.22945	1.09639	0.29685	-
WaveNet Oord et al. [2016]	0.17783	0.84973	0.27339	-
eTS Angelov and Filev [2004]	0.18750	0.89595	<b>0.25613</b>	4
Simpl_eTS Angelov and Filev [2005]	0.20622	0.98540	0.28118	45
exTS Angelov and Zhou [2006]	<b>0.16995</b>	<b>0.81211</b>	0.25916	5
ePL Lima et al. [2010]	0.22578	1.07888	0.39487	1
eMG Lemos et al. [2010]	0.28605	1.36686	0.51978	176
ePL+ Maciel et al. [2012]	0.21503	1.02751	0.36951	1
ePL-KRLS-DISCO Alves and de Aguiar [2021]	0.21213	1.01365	0.36978	20
NMR	0.27135	1.29663	0.38104	8
NTSK (RLS)	0.20606	0.98463	0.34618	1
NTSK (wRLS)	0.22261	1.06370	0.38723	2
GEN-NMR	0.19319	0.92315	<b>0.26033</b>	19
GEN-NTSK (RLS)	0.26105	1.24740	0.45110	1
GEN-NTSK (wRLS)	0.21812	1.04229	0.37640	19
R-NMR	0.26611	1.27157	0.36162	-
R-NTSK	0.20941	1.00066	0.35864	-
RF-NTSK	<b>0.18351</b>	<b>0.87687</b>	0.30299	-

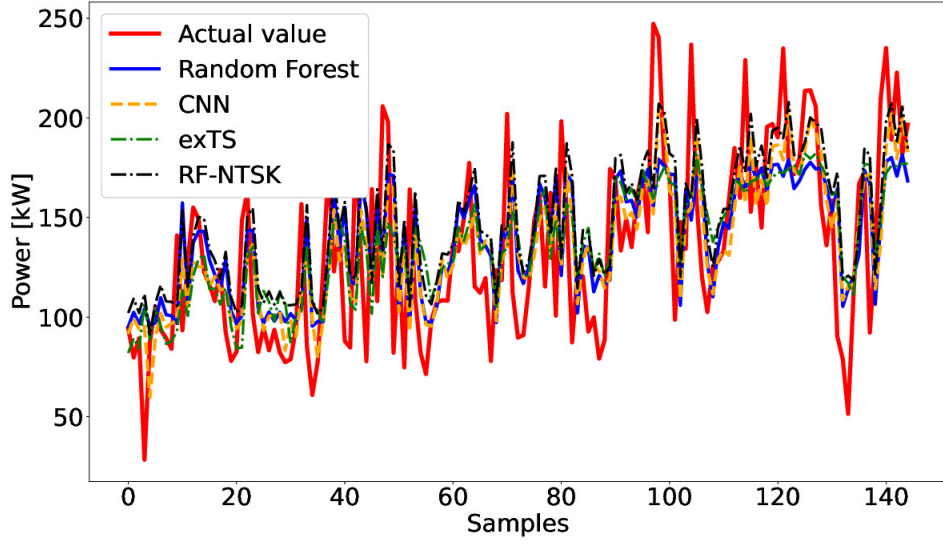


Figure 5: Graphic of predictions for Yulara 1

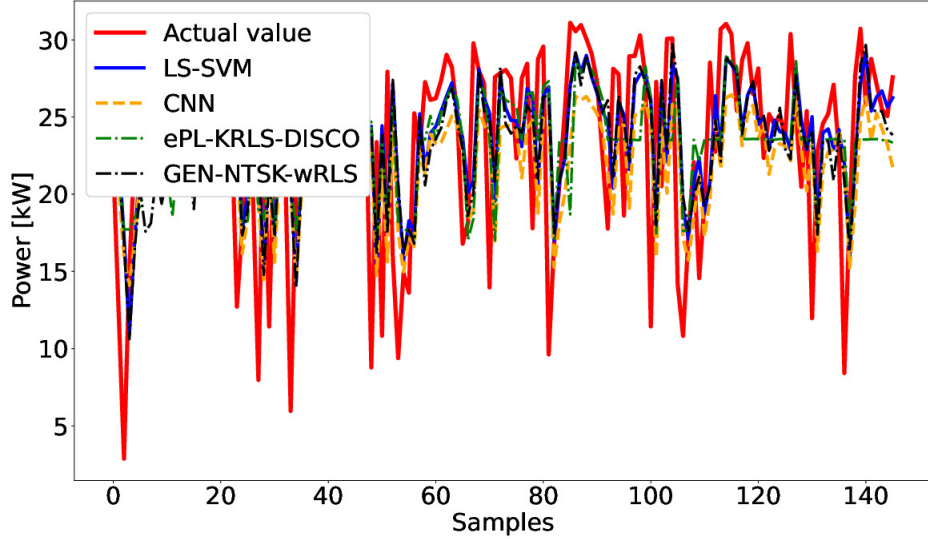


Figure 6: Graphic of predictions for Yulara 5

all models, and eMG had 372 final rules, the second-highest ones. Figure 6 presents the best predictions of each class for the Yulara 5 time series.

#### 4.4 Rules and Interpretability

A key advantage of genetic-based approaches is their ability to optimize the trade-off between accuracy and interpretability. For instance, the PV energy dataset contains numerous attributes. The GEN-NTSK-wRLS method selected six out of the twelve attributes, prioritizing those that most effectively contributed to predictive performance. This demonstrates one of the primary strengths of genetic algorithms: they can uncover hidden correlations between the target variable and the attributes, which may not be immediately evident through simple correlation analysis. As a

Table 6: Simulations’ results for the Yulara 5 PV panel

Model	NRMSE	NDEI	MAPE	Rules
KNN Fix and Hodges [1951]	0.23408	1.10290	0.33711	-
Regression Tree Breiman et al.	0.21492	1.01262	0.29218	-
Random Forest Ho [1995]	0.21306	1.00388	0.28702	-
SVM Cortes and Vapnik [1995]	0.22354	1.05322	0.29446	-
LS-SVM Suykens and Vandewalle [1999]	<b>0.20783</b>	<b>0.97920</b>	<b>0.28330</b>	-
GBM Friedman [2001]	0.21769	1.02570	0.28887	-
XGBoost Chen and Guestrin [2016]	0.22848	1.07649	0.30705	-
LGBM Ke et al. [2017]	0.21589	1.01717	0.28938	-
MLP Rosenblatt [1958]	0.21564	1.01601	0.30108	-
CNN Fukushima [1980]	<b>0.21186</b>	<b>0.99821</b>	0.28915	-
RNN Hopfield [1982]	0.29585	1.39393	0.37098	-
LSTM Hochreiter and Schmidhuber [1997]	0.30403	1.43246	0.37513	-
GRU Chung et al. [2014]	0.22070	1.03985	<b>0.28804</b>	-
WaveNet Oord et al. [2016]	0.21745	1.02455	0.29647	-
eTS Angelov and Filev [2004]	0.21658	1.02046	0.28506	3
Simpl_eTS Angelov and Filev [2005]	0.22494	1.05983	0.29851	431
exTS Angelov and Zhou [2006]	0.20669	0.97386	0.28372	3
ePL Lima et al. [2010]	0.20992	0.98907	0.29031	1
eMG Lemos et al. [2010]	0.32813	1.54603	0.41719	372
ePL+ Maciel et al. [2012]	0.20917	0.98555	0.28964	4
ePL-KRLS-DISCO Alves and de Aguiar [2021]	<b>0.20501</b>	<b>0.96595</b>	<b>0.28255</b>	20
NMR	0.32884	1.54935	0.39332	2
NTSK (RLS)	0.22291	1.05029	0.31533	1
NTSK (wRLS)	0.21398	1.00818	0.28825	5
GEN-NMR	0.29698	1.39928	0.36355	15
GEN-NTSK (RLS)	0.22080	1.04035	0.29857	1
GEN-NTSK (wRLS)	<b>0.20625</b>	<b>0.97176</b>	0.28503	15
R-NMR	0.36554	1.72230	0.42459	-
R-NTSK	0.20632	0.97209	<b>0.27714</b>	-
RF-NTSK	0.20749	0.97761	0.27978	-

result, the model identified a more concise rule-based structure with fewer rules, enhancing the analysis by focusing on the attributes that most significantly influence the outcomes.

Table 7: Rules of GEN-NTSK-wRLS for Alice 1A with four rules

Rule	Diffuse Radiation	Rainfall	Wind Direction	Current	Power	Global Radiation	Next Power
1	57.67 (27.35)	0.07 (0.20)	24.22 (18.12)	5.04 (0.85)	2.48 (0.49)	301.66 (69.41)	[-2.56, -1.37]
2	61.40 (37.21)	0.56 (2.41)	31.20 (15.20)	4.48 (1.07)	2.18 (0.64)	264.34 (88.11)	[-1.37, -0.18]
3	54.35 (35.91)	0.46 (2.45)	31.33 (15.58)	4.54 (1.11)	2.24 (0.57)	270.44 (78.31)	[-0.18, 1.01]
4	79.98 (34.09)	0.96 (3.43)	27.92 (15.82)	3.82 (1.33)	1.79 (0.76)	218.76 (95.23)	[1.01, 2.20]

#### 4.5 Discussion

Regarding the proposed models, NTSK with feature selection approach achieved superior performance compared to the other proposed models. This suggests that feature selection is effective in addressing the challenges posed by noisy datasets. For eFSs, the eTS and exTS models outperformed the rest of eFSs. Notably, Simpl\_eTS generated the highest number of rules in many simulations. Regarding DL models, CNN exhibited superior performance for the renewable energy datasets, achieving the lowest errors. Finally, among the classical models, LS-SVM achieved the lowest errors for the renewable energy datasets.

The proposed approach for designing fuzzy rules offers two key advantages: simplicity and fewer hyperparameters. This simplicity translates to reduced training and testing times, making the proposed models well-suited for real-world applications requiring rapid implementation. Despite their simplicity and non-evolving structure, the proposed models achieved comparable or even superior error results compared to eFSs. Another notable advantage of the proposed models is that users can directly specify the desired number of rules, unlike most rule-based models in the literature. This feature allows users to customize the number of rules to balance accuracy and interpretability. Furthermore, the implementation of a genetic algorithm for attribute selection enhances the models’ robustness, enabling them to handle

diverse datasets more effectively by reducing errors and improving interpretability. Lastly, the ensemble approach contributes to reducing uncertainty in the results.

## 5 Conclusion

This work introduces new data-driven fuzzy inference systems (NFISiS) for time series forecasting. NFISiS includes a series of fuzzy models, including: the new Mamdani classifier (NMC), new Mamdani regressor (NMR) and the new Takagi-Sugeno-Kang (NTSK), GEN-NMR, GEN-NTSK, R-NMR, R-NTSK. For the NTSK, two adaptive filtering are implemented, the Recursive Least Squares (RLS) and the weighted Recursive Least Squares (wRLS), producing the NTSK (RLS) and NTSK (wRLS). The following advantages of the proposed model can be highlighted: (i) a novel data-driven mechanism for designing Mamdani and TSK rules that provides reduced complexity, higher autonomy and accuracy, and less hyperparameters; (ii) the implementation of feature selection approaches that enhances the models' ability to handle large datasets, optimize their performance, increase interpretability, and avoid overfitting. The models are applied solar energy datasets. Their performance are evaluated in terms of errors and the number of rules. GEN-NTSK and RF-NTSK obtained the lowest error among the proposed models.

One of the main advantages of NTSK concerning the conventional TSK is their increased interpretability, as the polynomial functions of the consequent part can be replaced by the expected variation of the target value when presenting the rule-based structure. As the demand for mechanisms ensuring the safe operation of critical systems continues to rise, the models proposed in this work are well-suited for implementation as control tools due to their reliability and simplicity. Their application can support decision-making across various domains, such as finance, by improving system performance and optimizing monetary outcomes. For future research, we recommend exploring alternative fuzzy set types and developing a method for automatically selecting the optimal fuzzy set shape. Additionally, a post-processing stage for fine-tuning fuzzy set parameters could be investigated. Other algorithms, such as kernel recursive least squares (KRLS), may also be explored for estimating the parameters of the consequent part. Finally, we suggest further evaluating the proposed models on diverse datasets, including those with higher dimensionality and increased uncertainty, to compare their performance with type-2 fuzzy sets.

## References

- Ajay Shrestha and Ausif Mahmood. Review of deep learning algorithms and architectures. *IEEE Access*, 7:53040–53065, 2019. doi:<https://doi.org/10.1109/ACCESS.2019.2912200>.
- Xizhao Wang, Yanxia Zhao, and Farhad Pourpanah. Recent advances in deep learning. *International Journal of Machine Learning and Cybernetics*, 11:747–750, 2020. doi:<https://doi.org/10.1007/s13042-020-01096-5>.
- Arun Rai. Explainable AI: From black box to glass box. *Journal of the Academy of Marketing Science*, 48:137–141, 2020. doi:<https://doi.org/10.1007/s11747-019-00710-5>.
- Ebrahim H Mamdani. Application of fuzzy algorithms for control of simple dynamic plant. In *Proceedings of the Institution of Electrical Engineers*, volume 121, pages 1585–1588. IET, 1974. doi:<https://doi.org/10.1049/piee.1974.0328>.
- Tomohiro Takagi and Michio Sugeno. Fuzzy identification of systems and its applications to modeling and control. *IEEE Transactions on Systems, Man, and Cybernetics*, SMC-15(1):116–132, 1985. doi:<https://doi.org/10.1109/TSMC.1985.6313399>.
- Michio Sugeno and GT Kang. Structure identification of fuzzy model. *Fuzzy Sets and Systems*, 28(1):15–33, 1988. doi:[http://dx.doi.org/10.1016/0165-0114\(88\)90113-3](http://dx.doi.org/10.1016/0165-0114(88)90113-3).
- George Bojadziev and Maria Bojadziev. *Fuzzy logic for business, finance, and management*, volume 23. World Scientific, 2007.
- Piotr S Szczepaniak and Paulo JG Lisboa. *Fuzzy systems in medicine*, volume 41. Physica, 2012.
- Radu-Emil Precup and Hans Hellendoorn. A survey on industrial applications of fuzzy control. *Computers in Industry*, 62(3):213–226, 2011. doi:<https://doi.org/10.1016/j.compind.2010.10.001>.
- Makoto Komiyama, Keitaro Yoshimoto, Masahiko Sisido, and Katsuhiko Ariga. Chemistry can make strict and fuzzy controls for bio-systems: DNA nanoarchitectonics and cell-macromolecular nanoarchitectonics. *Bulletin of the Chemical Society of Japan*, 90(9):967–1004, 2017. doi:<https://doi.org/10.1246/bcsj.20170156>.
- Patricia Melin, Olivia Mendoza, and Oscar Castillo. Face recognition with an improved interval type-2 fuzzy logic Sugeno integral and modular neural networks. *IEEE Transactions on Systems, Man, and Cybernetics-Part A: Systems and Humans*, 41(5):1001–1012, 2011. doi:<https://doi.org/10.1109/TSMCA.2010.2104318>.

- Andre Lemos, Waldir Caminhas, and Fernando Gomide. Adaptive fault detection and diagnosis using an evolving fuzzy classifier. *Information Sciences*, 220:64–85, 2013. doi:<https://doi.org/10.1016/j.ins.2011.08.030>.
- Kaika Sa Teles Rocha Alves, Caian Dutra de Jesus, and Eduardo Pestana de Aguiar. A new Takagi–Sugeno–Kang model for time series forecasting. *Engineering Applications of Artificial Intelligence*, 133:108155, 2024. doi:<https://doi.org/10.1016/j.engappai.2024.108155>.
- Kaika Sa Teles Rocha Alves, Rosangela Ballini, and Eduardo Pestana de Aguiar. Financial Series Forecasting: A New Fuzzy Inference System for Crisp Values and Interval-Valued Predictions. *Computational Economics*, pages 1–49, 2024. doi:<https://doi.org/10.1007/s10614-024-10670-w>.
- Rizgar Zebari, Adnan Abdulazeez, Diyar Zeebaree, Dilovan Zebari, and Jwan Saeed. A comprehensive review of dimensionality reduction techniques for feature selection and feature extraction. *Journal of Applied Science and Technology Trends*, 1(1):56–70, 2020. doi:<https://doi.org/10.38094/jastt1224>.
- Adel Sabry Eesa, Zeynep Orman, and Adnan Mohsin Abdulazeez Brifcani. A novel feature-selection approach based on the cuttlefish optimization algorithm for intrusion detection systems. *Expert Systems with Applications*, 42(5): 2670–2679, 2015. doi:<https://doi.org/10.1016/j.eswa.2014.11.009>.
- Yifei Mao and Yuansheng Yang. A wrapper feature subset selection method based on randomized search and multilayer structure. *BioMed Research International*, 2019(1):9864213, 2019. doi:<https://doi.org/10.1155/2019/9864213>.
- Ayesha Sohail. Genetic algorithms in the fields of artificial intelligence and data sciences. *Annals of Data Science*, 10(4):1007–1018, 2023. doi:<https://doi.org/10.1007/s40745-021-00354-9>.
- Rana Forsati, Alireza Moayedikia, Richard Jensen, Mehrnoush Shamsfard, and Mohammad Reza Meybodi. Enriched ant colony optimization and its application in feature selection. *Neurocomputing*, 142:354–371, 2014. doi:<https://doi.org/10.1016/j.neucom.2014.03.053>.
- Isabelle Guyon and André Elisseeff. An introduction to variable and feature selection. *Journal of Machine Learning Research*, 3(Mar):1157–1182, 2003.
- Hui-Huang Hsu, Cheng-Wei Hsieh, and Ming-Da Lu. Hybrid feature selection by combining filters and wrappers. *Expert Systems with Applications*, 38(7):8144–8150, 2011. doi:<https://doi.org/10.1016/j.eswa.2010.12.156>.
- Verónica Bolón-Canedo and Amparo Alonso-Betanzos. Ensembles for feature selection: A review and future trends. *Information Fusion*, 52:1–12, 2019. doi:<https://doi.org/10.1016/j.inffus.2018.11.008>.
- Xibin Dong, Zhiwen Yu, Wenming Cao, Yifan Shi, and Qianli Ma. A survey on ensemble learning. *Frontiers of Computer Science*, 14:241–258, 2020. doi:<https://doi.org/10.1007/s11704-019-8208-z>.
- Alba Alcañiz, Daniel Grzebyk, Hesam Ziar, and Olindo Isabella. Trends and gaps in photovoltaic power forecasting with machine learning. *Energy Reports*, 9:447–471, 2023. doi:<https://doi.org/10.1016/j.egy.2022.11.208>.
- Gilles Notton, Marie-Laure Nivet, Cyril Voyant, Christophe Paoli, Christophe Darras, Fabrice Motte, and Alexis Fouilloy. Intermittent and stochastic character of renewable energy sources: Consequences, cost of intermittence and benefit of forecasting. *Renewable and Sustainable Energy Reviews*, 87:96–105, 2018. doi:<https://doi.org/10.1016/j.rser.2018.02.007>.
- Martin János Mayer and Gyula Gróf. Extensive comparison of physical models for photovoltaic power forecasting. *Applied Energy*, 283:116239, 2021. doi:<https://doi.org/10.1016/j.apenergy.2020.116239>.
- Can Wan, Jian Zhao, Yonghua Song, Zhao Xu, Jin Lin, and Zechun Hu. Photovoltaic and solar power forecasting for smart grid energy management. *CSEE Journal of Power and Energy Systems*, 1(4):38–46, 2015. doi:<https://doi.org/10.17775/CSEEJPES.2015.00046>.
- Florian Barbieri, Sumedha Rajakaruna, and Arindam Ghosh. Very short-term photovoltaic power forecasting with cloud modeling: A review. *Renewable and Sustainable Energy Reviews*, 75:242–263, 2017. doi:<https://doi.org/10.1016/j.rser.2016.10.068>.
- Utpal Kumar Das, Kok Soon Tey, Mehdi Seyedmahmoudian, Saad Mekhilef, Moh Yamani Idna Idris, Willem Van Deventer, Bend Horan, and Alex Stojcevski. Forecasting of photovoltaic power generation and model optimization: A review. *Renewable and Sustainable Energy Reviews*, 81:912–928, 2018. doi:<https://doi.org/10.1016/j.rser.2017.08.017>.
- Muhammad Munsif, Min Ullah, U Fath, Samee Ullah Khan, Noman Khan, and Sung Wook Baik. CT-NET: A Novel Convolutional Transformer-Based Network for Short-Term Solar Energy Forecasting Using Climatic Information. *Computer Systems Science & Engineering*, 47(2), 2023. doi:<https://doi.org/10.32604/csse.2023.038514d>.
- Nur Liyana Mohd Jailani, Jeeva Kumaran Dhanasegaran, Gamal Alkaws, Ammar Ahmed Alkahtani, Chen Chai Phing, Yahia Baashar, Luiz Fernando Capretz, Ali Q Al-Shetwi, and Sieh Kiong Tiong. Investigating the Power of LSTM-Based Models in Solar Energy Forecasting. *Processes*, 11(5):1382, 2023. doi:<https://doi.org/10.3390/pr11051382>.

- Amith Khandakar, Muhammad EH Chowdhury, Monzure Khoda Kazi, Kamel Benhmed, Farid Touati, Mohammed Al-Hitmi, and Antonio Jr SP Gonzales. Machine learning based photovoltaics (PV) power prediction using different environmental parameters of Qatar. *Energies*, 12(14):2782, 2019. doi:<https://doi.org/10.3390/en12142782>.
- Daniel O’Leary, Joel Kubby, et al. Feature selection and ANN solar power prediction. *Journal of Renewable Energy*, 2017, 2017. doi:<https://doi.org/10.1155/2017/2437387>.
- Neetan Sharma, Vinod Puri, Shubham Mahajan, Laith Abualigah, Raed Abu Zitar, and Amir H Gandomi. Solar power forecasting beneath diverse weather conditions using GD and LM-artificial neural networks. *Scientific Reports*, 13(1):8517, 2023. doi:<https://doi.org/10.1038/s41598-023-35457-1>.
- Hong-Tzer Yang, Chao-Ming Huang, Yann-Chang Huang, and Yi-Shiang Pai. A weather-based hybrid method for 1-day ahead hourly forecasting of PV power output. *IEEE Transactions on Sustainable Energy*, 5(3):917–926, 2014. doi:<https://doi.org/10.1109/TSTE.2014.2313600>.
- Stefan Preda, Simona-Vasilica Oprea, Adela Bâra, and Anda Belciu. PV forecasting using support vector machine learning in a big data analytics context. *Symmetry*, 10(12):748, 2018. doi:<https://doi.org/10.3390/sym10120748>.
- Yanting Li, Yong He, Yan Su, and Lianjie Shu. Forecasting the daily power output of a grid-connected photovoltaic system based on multivariate adaptive regression splines. *Applied Energy*, 180:392–401, 2016. doi:<https://doi.org/10.1016/j.apenergy.2016.07.052>.
- Abinet Tesfaye Eseye, Jianhua Zhang, and Dehua Zheng. Short-term photovoltaic solar power forecasting using a hybrid Wavelet-PSO-SVM model based on SCADA and meteorological information. *Renewable Energy*, 118:357–367, 2018. doi:<https://doi.org/10.1016/j.renene.2017.11.011>.
- William VanDeventer, Elmira Jamei, Gokul Sidarth Thirunavukkarasu, Mehdi Seyedmahmoudian, Tey Kok Soon, Ben Horan, Saad Mekhilef, and Alex Stojcevski. Short-term PV power forecasting using hybrid GASVM technique. *Renewable Energy*, 140:367–379, 2019. doi:<https://doi.org/10.1016/j.renene.2019.02.087>.
- Fang Liu, Ranran Li, Yong Li, Ruifeng Yan, and Tapan Saha. Takagi–Sugeno fuzzy model-based approach considering multiple weather factors for the photovoltaic power short-term forecasting. *IET Renewable Power Generation*, 11(10):1281–1287, 2017. doi:<https://doi.org/10.1049/iet-rpg.2016.1036>.
- Ling Liu, Fang Liu, and Yuling Zheng. A novel ultra-short-term PV power forecasting method based on DBN-based Takagi-Sugeno fuzzy model. *Energies*, 14(20):6447, 2021. doi:<https://doi.org/10.3390/en14206447>.
- Mahmoud Ghofrani, Mohadeseh Ghayekhloo, and Rasool Azimi. A novel soft computing framework for solar radiation forecasting. *Applied Soft Computing*, 48:207–216, 2016. doi:<https://doi.org/10.1016/j.asoc.2016.07.022>.
- Edward W Law, Abhnil A Prasad, Merlinde Kay, and Robert A Taylor. Direct normal irradiance forecasting and its application to concentrated solar thermal output forecasting—A review. *Solar Energy*, 108:287–307, 2014. doi:<https://doi.org/10.1016/j.solener.2014.07.008>.
- SM Azimi and H Miar-Naimi. Designing programmable current-mode Gaussian and bell-shaped membership function. *Analog Integrated Circuits and Signal Processing*, 102(2):323–330, 2020. doi:<https://doi.org/10.1007/s10470-019-01567-y>.
- Samuel Sanford Shapiro and Martin B Wilk. An analysis of variance test for normality (complete samples). *Biometrika*, 52(3/4):591–611, 1965. doi:<https://doi.org/10.2307/2333709>.
- David A Dickey and Wayne A Fuller. Likelihood ratio statistics for autoregressive time series with a unit root. *Econometrica: Journal of the Econometric Society*, pages 1057–1072, 1981. doi:<https://doi.org/10.2307/1912517>.
- Evelyn Fix and JL Hodges. Discriminatory analysis, nonparametric discrimination. Technical report, Consistency Properties. Technical Report 4, USAF School of Aviation Medicine, Randolph Field., 1951.
- Leo Breiman, Jerome H Friedman, Richard A Olshen, and Charles J Stone. Classification and regression trees (Wadsworth, Belmont, CA). *ISBN-13*, pages 978–0412048418.
- Tin Kam Ho. Random decision forests. In *Proceedings of 3rd International Conference on Document Analysis and Recognition*, volume 1, pages 278–282. IEEE, 1995. doi:<https://doi.org/10.1109/ICDAR.1995.598994>.
- Corinna Cortes and Vladimir Vapnik. Support-vector networks. *Machine Learning*, 20:273–297, 1995. doi:<https://doi.org/10.1007/BF00994018>.
- Johan AK Suykens and Joos Vandewalle. Least squares support vector machine classifiers. *Neural Processing Letters*, 9:293–300, 1999. doi:<https://doi.org/10.1023/A:1018628609742>.
- Jerome H Friedman. Greedy function approximation: a gradient boosting machine. *Annals of Statistics*, pages 1189–1232, 2001. doi:<https://doi.org/10.1214/aos/1013203451>.

- Tianqi Chen and Carlos Guestrin. XGBoost: A scalable tree boosting system. In *Proceedings of the 22nd ACM SIGKDD International Conference on Knowledge Discovery and Data Mining*, pages 785–794, 2016. doi:https://doi.org/10.1145/2939672.2939785.
- Guolin Ke, Qi Meng, Thomas Finley, Taifeng Wang, Wei Chen, Weidong Ma, Qiwei Ye, and Tie-Yan Liu. LightGBM: A highly efficient gradient boosting decision tree. *Advances in Neural Information Processing Systems*, 30, 2017. doi:https://doi.org/10.1007/s11280-022-01033-2.
- Frank Rosenblatt. The perceptron: a probabilistic model for information storage and organization in the brain. *Psychological Review*, 65(6):386, 1958. doi:https://psycnet.apa.org/doi/10.1037/h0042519.
- Kunihiko Fukushima. Neocognitron: A self-organizing neural network model for a mechanism of pattern recognition unaffected by shift in position. *Biological Cybernetics*, 36(4):193–202, 1980. doi:https://doi.org/10.1007/BF00344251.
- John J Hopfield. Neural networks and physical systems with emergent collective computational abilities. *Proceedings of the National Academy of Sciences*, 79(8):2554–2558, 1982. doi:https://doi.org/10.1073/pnas.79.8.2554.
- Sepp Hochreiter and Jürgen Schmidhuber. Long short-term memory. *Neural Computation*, 9(8):1735–1780, 1997. doi:https://doi.org/10.1162/neco.1997.9.8.1735.
- Junyoung Chung, Caglar Gulcehre, KyungHyun Cho, and Yoshua Bengio. Empirical evaluation of gated recurrent neural networks on sequence modeling. *arXiv preprint arXiv:1412.3555*, 2014. doi:https://doi.org/10.48550/arXiv.1412.3555.
- Aaron van den Oord, Sander Dieleman, Heiga Zen, Karen Simonyan, Oriol Vinyals, Alex Graves, Nal Kalchbrenner, Andrew Senior, and Koray Kavukcuoglu. Wavenet: A generative model for raw audio. *arXiv preprint arXiv:1609.03499*, 2016. doi:https://doi.org/10.48550/arXiv.1609.03499.
- Plamen P Angelov and Dimitar P Filev. An approach to online identification of Takagi-Sugeno fuzzy models. *IEEE Transactions on Systems, Man, and Cybernetics, Part B (Cybernetics)*, 34(1):484–498, 2004. doi:https://doi.org/10.1109/TSMCB.2003.817053.
- Plamen Angelov and Dimitar Filev. Simpl\_eTS: A simplified method for learning evolving Takagi-Sugeno fuzzy models. In *The 14th IEEE International Conference on Fuzzy Systems, 2005. FUZZ'05.*, pages 1068–1073. IEEE, 2005. doi:https://doi.org/10.1109/FUZZY.2005.1452543.
- Plamen Angelov and Xiaowei Zhou. Evolving fuzzy systems from data streams in real-time. In *2006 International Symposium on Evolving Fuzzy Systems*, pages 29–35. IEEE, 2006. doi:https://doi.org/10.1109/ISEFS.2006.251157.
- E Lima, M Hell, R Ballini, and F Gomide. Evolving fuzzy modeling using participatory learning. *Evolving Intelligent Systems: Methodology and Applications*, pages 67–86, 2010. doi:https://doi.org/10.1002/9780470569962.ch4.
- Andre Lemos, Walmir Caminhas, and Fernando Gomide. Multivariable Gaussian evolving fuzzy modeling system. *IEEE Transactions on Fuzzy Systems*, 19(1):91–104, 2010. doi:https://doi.org/10.1109/TFUZZ.2010.2087381.
- Leandro Maciel, Fernando Gomide, and Rosangela Ballini. An enhanced approach for evolving participatory learning fuzzy modeling. In *2012 IEEE Conference on Evolving and Adaptive Intelligent Systems*, pages 23–28. IEEE, 2012. doi:https://doi.org/10.1109/EAIS.2012.6232799.
- Kaike Sa Teles Rocha Alves and Eduardo Pestana de Aguiar. A novel rule-based evolving fuzzy system applied to the thermal modeling of power transformers. *Applied Soft Computing*, 112:107764, 2021. doi:https://doi.org/10.1016/j.asoc.2021.107764.